Probing helix propensity of monomers within a helical oligomer

Christel Dolain[†], Jean-Michel Léger[‡], Nicolas Delsuc[†], Heinz Gornitzka[§], and Ivan Huc[†¶]

[†]Institut Européen de Chimie et Biologie, 2 Rue Robert Escarpit, F-33607 Pessac, France; [‡]Laboratoire de Pharmacochimie, 146 Rue Léo Saignat, F-33076 Bordeaux, France; and [§]Laboratoire d'Hétérochimie Fondamentale et Appliquée, Université Paul Sabatier, 118 Route de Narbonne, 31062 Toulouse Cedex 4, France

Edited by Jack Halpern, University of Chicago, Chicago, IL, and approved September 23, 2005 (received for review July 22, 2005)

A simple strategy is proposed to assess the propensity of a given monomer to follow or not follow a particular helical scheme and to study helix reversal phenomena within helical oligomers. It consists of placing a monomer having a low helix propensity between two conformationally stable helical segments. Helix reversion then occurs preferentially at the site of this monomer, leading to the formation of isomers having P (right-handed) or M (left-handed) helicities at each of the two helical segments. The proportion between the P-P/M-M and P-M isomers is indicative of the stereochemical relations between the inserted monomer and the helical frame. Thus, xylylene or carboxylic acid anhydride spacers have been introduced between two helical oligoamides of 8-amino-2-quinolinecarboxylic acid. Both these spacers presumably lack some of the structural features that confer quinoline units with a high helix propensity. Only one species is observed in solution in the case of an anhydride spacer. This species was shown by x-ray crystallography to be a racemic mixture of P-P and M-M helices. Unexpectedly, the anhydride is consistently incorporated within helical oligoamides. For the xylylene spacer, the P-P/M-M racemate and P-M *meso* compound are in equal proportions in chloroform, showing that this spacer does not have a propensity to adopt any helical conformation in this solvent. However, the equilibria between the various isomers are shifted in toluene, where one species largely prevails. This species was shown by x-ray crystallography to be the P-P/M-M racemate. Molecular dynamics simulations are consistent with these solution data.

conformation analysis | folding | helices

Molecular helices are one of the major structural motifs of natural and synthetic polymers and oligomers (1–7). A fundamental property of a molecular helix is the average length over which it keeps its right-handed (P) or left-handed (M) integrity: the length over which neither uncoiling nor reversal of helix handedness occurs. This parameter is important in structural biology because it reflects the stability of, for example, α-helical peptides; it is also important in material science because it determines the limit of chiral amplification that a given helical polymeric chain may reach (1, 6). Helical integrity may also be useful to remotely control the stereochemistry of a reaction (8). For example, in a helical polymer, a single chiral residue may induce a local conformational preference for a particular handedness. This local preference is propagated and amplified by the helical integrity of the polymer until a partial uncoiling or helix reversal occurs. The average length over which a helix handedness keeps its integrity is determined by a combination of local conformational preferences in the helix backbone as well as intramolecular and solvent-driven interactions that define the helix propensity associated with the monomers (1–7). Long-range intermolecular helix–helix interactions and helix bundling have also been shown contribute to helix stability (9–13). The balance between these factors is subtle, and helix propensity is difficult to predict and characterize. Calculations may provide some information about the structure of a helix reversal center (14). However, to the best of our knowledge, such sites have not been characterized by experimental means, mainly because reversal centers are labile and do not normally reside at specific locations in a long helical chain.

Here, we propose a simple yet unexplored strategy to gain some insight into these phenomena. We anticipated that a monomer having a low helix propensity inserted between two stable helical segments would precisely define a site where helical reversion may occur, making it possible to structurally characterize such a site. Additionally, the extent of helix handedness inversion at this site allows us to probe the propensity of the added monomer to fold into a helix. Compounds **1**–**3** (Fig. 1) were designed and synthesized for the purpose of this study. These oligomers contain two octameric (**1**) or tetrameric (**2** and **3**) aromatic oligoamide segments of 8-amino-2-quinolinecarboxylic acid separated by a *meta*-xylylene spacer (**1** and **2**) or a carboxylic acid anhydride spacer (**3**). Quinolinecarboxamide oligomers (QCOs) adopt unusually stable helical conformations held by a network of hydrogen bonds between amide protons and adjacent quinoline nitrogens, by repulsive electrostatic interactions between quinoline nitrogens and amide oxygens, and by extensive intramolecular aromatic stacking (7, 15–20). Thus, each tetrameric segment undergoes $\approx$1.5 helical turns, and each octameric segment undergoes $>$3 turns. As an illustration of the stability of these helical conformations, an octamer shows no sign of unfolding at 120°C in DMSO (15, 16). In contrast, the xylylene and anhydride spacers lack some of the features that ensure helix stability in QCOs. The xylylene unit contains sp3 carbons that interrupt conjugation throughout the oligomer and should perturb intramolecular aromatic stacking. It also lacks a hydrogen-bond acceptor in position 2 of the phenyl ring. The anhydride unit lacks a hydrogen-bond donor. One can thus reasonably expect that helix reversal in **1**–**3** should primarily take place at the spacer site. Each of the two QCO segments on either side of the spacer may be P or M, and the proportion of P-P (or its enantiomer M-M) and P-M diastereomer depends on the helix propensity of the spacer in between. As presented in the following, we have used NMR, x-ray crystallography, and molecular dynamics simulations to characterize helix inversion and to measure helix propensity of xylylene and anhydride spacers in the context of QCOs.

Materials and Methods

NMR Studies. Four hundred megahertz ^{1}H NMR spectra were recorded with an Avance 400 NB US NMR spectrometer (Bruker, Ettlingen, Germany) by means of a 5-mm direct QNP

Conflict of interest statement: No conflicts declared.

This paper was submitted directly (Track II) to the PNAS office.

Abbreviations: P, right-handed; M, left-handed; QCO, quinolinecarboxamide oligomer; ROESY, rotating-frame Overhauser effect spectroscopy; NOE, nuclear Overhauser effect.

Data deposition: The atomic coordinates and structure factors of oligomers **1(Cl)$_2$**, **2**, and **3** have been deposited in the Cambridge Structural Database, Cambridge Crystallographic Data Centre, Cambridge CB2 1EZ, United Kingdom (CSD reference nos. 279125–279127).

¶To whom correspondence should be addressed. E-mail: i.huc@iecb.u-bordeaux.fr.

www.pnas.org/cgi/doi/10.1073/pnas.0506262102

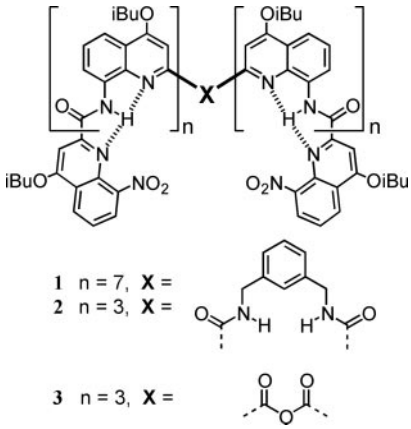

Fig. 1. Structures of oligomers **1**–**3**.

1H/X probe with gradient capabilities. The solvent signal was used as an internal reference for these spectra. Samples were not degassed. Rotating-frame Overhauser spectroscopy (ROESY) was used to study conformations at the helix inversion center with the following acquisition parameters: 90° pulse width and transmitter attenuation for the spin-lock pulses were calibrated, P1 = 13 μs, PL1 = 0 dB, spin-lock field strength = 4,807 Hz; 1,024(t2).512(t1) data points in States-TPPI mode with Z gradients selection and with clockwise spin-lock for mixing; relaxation delay of 2 s and 40 scans per increment; sweep width of 5,200 Hz in both dimensions; mixing time of 300 ms. Processing was done after a sine-bell multiplication in both dimensions and Fourier transformation in 1K.1K real points. Data processing was performed with XWIN-NMR software.

X-Ray Crystallography. A single crystal of compound $\mathbf{1(CL)_2}$ was mounted on an R-Axis Rapid diffractometer (Rigaku, Tokyo) equipped with a MM007 microfocus rotating anode generator with monochromatized Cu-Kα radiation (1.54178 Å). The data collection, unit cell refinement, and data reduction were performed by using the CRYSTALCLEAR software package. The positions of non-H atoms were determined by the program SHELXS 87, and the positions of the H atoms were deduced from coordinates of the non-H atoms and confirmed by Fourier synthesis. H atoms were included for structure factor calculations but not refined.

Single crystals of compounds **2** and **3** were mounted on Bruker-Nonius κ-CCD diffractometer with graphite monochromatized Mo-Kα radiation (0.71073 Å). The data collection was based on ϕ scans completed by ω scans. The final unit cell was determined on the basis of all of the collected frames. The data reduction was performed by using COLLECT software (Nonius). The positions of non-H atoms were determined by the program SHELXS 87 , and the positions of the H atoms were deduced from coordinates of the non-H atoms and confirmed by Fourier synthesis. H atoms were included for structure factor calculations but not refined.

Molecular Modeling. Molecular dynamics simulations of oligomer **1** were performed on an R10000 O2 workstation (Silicon Graphics, Mountain View, CA) using MACROMODEL 6.5 (Schrödinger). Stochastic dynamics simulations were run in the MACROMODEL version of the modified MM3* (1991 parameters) force field as implemented and completed in the MACROMODEL program at 300, 400, 500, and 600 K with GB/SA (generalized Born/surface area) solvation ($CHCl_3$), extended nonbonded distance cutoffs, constrained bond lengths, and a 1.5-fs time step. After a 2-ps initialization period, structures were sampled every 2 ps for 1 ns.

Synthetic Procedures. See the supporting information, which is published on the PNAS web site.

Results and Discussion

Solution Equilibrium Between P-P, M-M, and P-M Isomers. The presence of P-P/M-M and P-M isomers in **1**–**3** was first assessed by ^{1}H NMR spectroscopy. The P-P/M-M conformations possess a C_2 symmetry axis in their folded conformation, and the P-M species are expected to possess an inversion center. Both species should thus show the same number of signals. For example, in **1**, both P-P/M-M and P-M isomers are expected to show 7 different signals for hydrogen-bonded aromatic amide protons. Indeed, the NMR spectrum of **1** in $CHCl_3$ shows 14 resonances in the hydrogen-bonded amide region (10.8–11.2 ppm) with almost

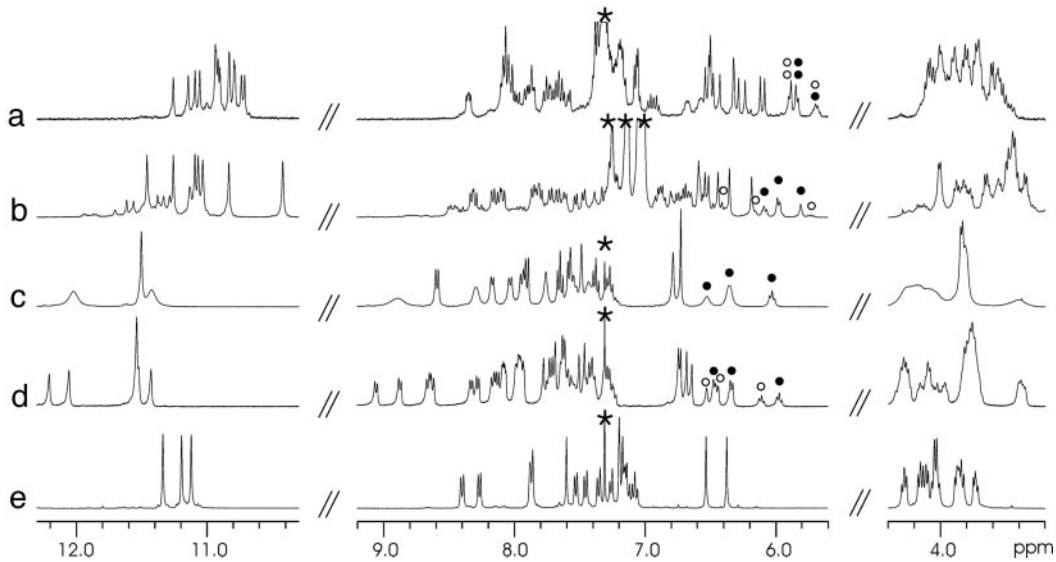

Fig. 2. Part of the 400-MHz ^{1}H NMR spectra of oligomers **1**, **2**, and **3** showing the signals of amide (10.3–12.3 ppm) and aromatic (5.6–9.1 ppm) protons. (*a*) **1** in $CDCl_3$ at 25°C. (*b*) **1** in toluene-d_8 at 25°C. (*c*) **2** in $CDCl_3$ at 25°C. (*d*) **2** in $CDCl_3$ at −20°C. (*e*) **3** in $CDCl_3$ at 25°C. The asterisks mark signals of residual hydrogenated solvent. The open and filled circles mark signals of the phenyl ring for P-M and P-P/M-M isomers.

equal intensities (Fig. 2*a*). Because the oligoamide segments are consistently folded under such conditions, these signals can be assigned on the one hand to the P-P/M-M enantiomers and on the other hand to the P-M diastereomer in which a helix reversal occurs at the spacer site. The equilibrium between the two species is slow on the NMR time scale, as expected for octameric QCOs (15–18). That the two species are in identical proportions indicates that the free energy of helix reversal of a single segment, ΔG_r, is close to zero in this compound. The xylylene spacer completely interrupts the helicity of QCOs, and its two helical segments possess unrelated handedness. Using the sergeant and soldier analogy proposed by Green *et al.* (21), the xylylene spacer behaves as a highly undisciplined soldier: It has a negligible helix propensity in the context of QCOs.

In chloroform, the signals of the two species are observed in the same regions and partly overlap, suggesting that the two helical segments on either side of the xylylene spacer are in a similar environment regardless of whether they have identical (P-P/M-M) or opposite (P-M) handedness. This overlap of the signals prevented a direct assignment of the spectra. Nevertheless, signals of protons belonging to the *meta*-xylylene unit were clearly identified at 5.6–6.0 ppm (Fig. 2*a*). The racemic helices (P-P/M-M) and the *meso* helix (P-M) are also in equal proportions in numerous other solvents (not shown) (e.g., chlorinated CD_2Cl_2 and CCl_4 or more polar solvents such as tetrahydrofuran-d_8, acetone-d_6, and DMSO-d_6), which shows that the equilibrium between the two species is not significantly affected in a polar environment.

The shorter oligomer **2** behaves in a similar way. Near 25°C, the equilibrium between the P-P/M-M and P-M diastereomers is fast on the NMR time scale, and the ^{1}H NMR spectrum in $CDCl_3$ shows only one set of broadened signals. Coalescence between the signals of P-P/M-M and P-M helices is thus reached at room temperature (Fig. 2*c*). Upon cooling to −20°C, this equilibrium becomes slow on the NMR time scale, and the broad signals split into two sets of sharp signals in almost identical proportions (Fig. 2*d*). As for oligomer **1**, the xylylene spacer completely interrupts the helicity of QCOs, and its two helical segments possess unrelated handedness.

However, the spectrum of oligomer **1** in toluene-d_8 at room temperature (Fig. 2*b*) shows that, in this solvent, the equilibrium is shifted to a ratio of 9:1 between the two types of helices. The same is observed for oligomer **2** in toluene at low temperature (not shown). Unlike in $CDCl_3$, the chemical shifts of the signals belonging to the two species differ significantly: The signals of the major species (e.g., amide resonances) are shifted up-field from those of the minor species, suggesting that ring current effects from intramolecular aromatic stacking are stronger in the major isomer. Toluene apparently favors intramolecular aromatic stacking, which results in the predominance of one species. It might be hypothesized that aromatic stacking is more extensive in the P-P/M-M isomers than in the *meso* helix, and, thus, a tentative assignment of the major signals to the P-P/M-M racemate might be proposed. One may also note that some monomers specifically stabilize inversion centers (18). In fact, NMR does not provide conclusive evidence in this respect.

To understand the change of P-P/M-M vs. P-M distribution in toluene, NMR spectra were recorded in three other aromatic solvents: C_6D_6, C_6D_5Br, and $C_6D_5NO_2$. It was found that $\log(K)$ (with K = [P-P/M-M]/[P-M]) increases linearly with the absolute hardness, η, of the solvent (22). The values of K span less than one order of magnitude, which is far less spectacular than effects recently reported about the unfolding rate of helical ethynylhelicene oligomers (23). It nevertheless suggests that secondary interactions between the helices and the solvent play a role in governing the P-P/M-M vs. P-M distribution.

In the case of anhydride **3**, the ^{1}H NMR spectrum in $CDCl_3$ shows only one set of sharp signals spread over a large range of chemical shifts (Fig. 2*e*). Amide protons are deshielded beyond 11 ppm, and aromatic protons are strongly shielded, consistent with tight contacts between aromatic rings of the two helical segments. The signals assigned to the OCH_2 groups of the side chains display diastereotopic patterns even at room temperature, showing that the rate of inversion of the helix is slow on the NMR time scale, even though the two helical segments are tetrameric QCOs. That only one species prevails in solution implies that both helical segments generally undergo helix inversion in a single event, resulting in equilibrium either between P-P and M-M enantiomers or between degenerate P-M and M-P helices. This helix inversion presumably requires a higher energy barrier, and thus slower kinetics, than in the case of **2**, for which each tetrameric helical segment may undergo handedness inversion independently to yield another diastereomer. As confirmed by x-ray crystallographic analysis (see below), the species highly prominent in solutions of anhydride **3** can be assigned to the P-P/M-M racemate. It is not clear whether minor signals observed in the NMR spectrum (Fig. 2*e*) belong to the P-M diastereomer or to impurities. In any case, their proportion does not exceed 2%, which sets a lower limit of 9.6 kJ/mol for the free energy of conversion of P-P/M-M helices to P-M helices. Thus, the anhydride unit unexpectedly appears to be a very obedient soldier.

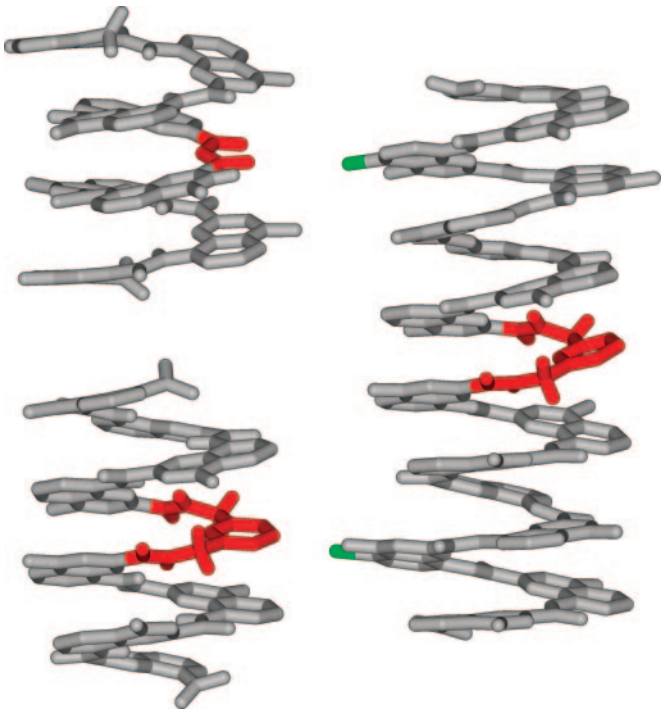

Fig. 3. Side views of the crystal structures of **1(Cl)$_2$** (*Right*), **2** (*Lower Left*), and **3** (*Upper Left*). Isobutyl chains, included solvent molecules, and hydrogen atoms are omitted for clarity, except for amide and benzylic hydrogens. The xylylene and anhydride spacers are shown in red; chlorine atoms are shown in green.

Crystallographic Assignment of the P-P/M-M Isomers. Crystals of **3** were grown over a few days upon diffusion of *n*-hexane into a chloroform solution. Because only one diastereomer is highly prominent in solution, we expected this species only to crystallize. X-ray diffraction analysis revealed that the crystals contain racemic P-P/M-M helices (Fig. 3), suggesting that it is indeed this form that dominates in solution. The crystal is centrosymmetric, and the asymmetric unit contains a full molecule of **3** (see the supporting information). This molecule does possess a

pseudo-C_2 symmetry axis, but it is not a crystallographic axis. In the central part of the molecule, the first quinoline ring at the C terminus of each tetrameric segment lies stacked face to face with the second quinoline ring at the C terminus of the other segment. These π–π interactions would not be possible in the P-M *meso* helix and probably contribute to the stability of the homochiral helical structure despite the lack of a hydrogen-bond donor within the anhydride spacer. It is likely that conformational preferences of the anhydride moiety also contribute to the stability of the homochiral helices. Specifically, electrostatic repulsions are expected between endocyclic quinoline nitrogens at the C terminus of each tetrameric segment and the adjacent sp^2 and sp^3 oxygen atoms of the anhydride. However, *s*-trans conformations about aryl-carbonyl linkages should be favored because repulsions involving the carbonyl sp^2 oxygen are stronger than those involving the sp^3 oxygen. Indeed, partial charge distribution, lone pair orientation, and bond lengths (in the structure of **3**, $d_{C=O}$ = 1.20 Å and d_{C-O} = 1.37 Å) all concur to enhance repulsions with sp^2 carbonyl oxygen atoms.

The structure of **2** was also characterized in the solid state (Fig. 3) by x-ray diffraction analysis (see the supporting information). Again, it shows a racemic mixture of P-P and M-M homochiral helices. As for **3**, the asymmetric unit of **2** contains a single full molecule with a pseudo-C_2 symmetry axis. The two central 2-quinolinecarboxamide groups are slightly tilted out of the plane of the *meta*-xylylene unit because of repulsions between the hydrogen in position 2 of the phenyl ring and the two neighbor amide protons. The phenyl group stacks with the next two quinoline rings in the sequence, between which it is sandwiched. However, sp^3 carbons interrupt conjugation throughout the oligomer and apparently perturb intramolecular aromatic stacking. It can be seen in the structure that the two methylene units, which are thicker than one aromatic ring, cause the quinoline rings above and below the phenyl ring to slightly diverge instead of being parallel and create a sort of bulge (Fig. 3). As initially intended, these perturbations probably result in weaker aromatic stacking with the xylylene unit than with an all-sp^2 system.

To determine whether the homochiral helices observed in the crystal structure of **2** are the major or the minor species observed in toluene solutions of this compound, NMR spectra were recorded immediately after dissolving crystals of **2** at −20°C. Unfortunately, these spectra showed not one but two sets of signals, which do not reflect the composition of the solid state but indicate that equilibrium between P-P/M-M and P-M helices has been reached within the few minutes necessary to record the spectra. Similar experiments were carried out with crystals of the longer oligomer **1**, which is expected to have much slower helix inversion kinetics (17). Crystals of **1** were grown from five different solvent combinations (diffusion of *n*-hexane into chloroform, toluene, benzene, chlorobenzene, and nitrobenzene solutions). Upon dissolving these crystals, NMR spectra showed that they indeed contain exclusively the diastereomer favored in toluene solution (see the supporting information). However, none of these crystals was suitable for x-ray diffraction analysis. Thus, the actual stereochemistry of the crystalline form of **1** remained unknown at this stage, although it seemed unlikely that the crystals of **1** would contain exclusively the major diastereomer of a toluene solution and that, at the same time, the P-P/M-M diastereomers observed in the crystals of shorter oligomer **2** would correspond to the minor isomer of a toluene solution.

We were finally able to lift these difficulties by using oligomer **1(Cl)$_2$**, which has the same structure as oligomer **1** except that it bears two chlorine atoms, each of them in position 5 of the third quinoline ring from either end of the sequence. Unlike crystals of **1**, which were all twinned, crystals of **1(Cl)$_2$** are unique and suitable for diffraction analysis (see the supporting information). The structure of **1(Cl)$_2$** is related to that of **2** and shows a racemic mixture of P-P and M-M homochiral helices. This compound has a molecular mass >4.2 kDa, and, to the best of our knowledge, its structure represents the largest x-ray structure of a synthetic foldamer to date. Upon redissolving crystals of **1(Cl)$_2$**, helix inversion is slow on the NMR time scale, and NMR spectra show one species that can be identified as the major species of toluene solution, consistent with the data collected with **1** and **2**. In summary, it was demonstrated that unlike other solvents tested, toluene favors a P-P/M-M racemate of homochiral helices at the expense of P-M *meso*-helices.

Conformations at the Helix Inversion Center. We anticipated that a monomer having a low helix propensity inserted between two stable helical segments would precisely define a site where helix handedness inversion may occur. As suggested by both solution and solid-state data, the highly flexible xylylene unit perturbs intramolecular aromatic stacking that ensures helix stability in QCOs. Helix reversion seems to occur preferentially at this site, leading to the formation of isomers having P or M helicities at each of the two helical segments on either side of the spacer. This fact makes it conceivable to structurally characterize such a site and, in particular, to determine the conformations adopted by the two phenyl–CH_2–NH bonds in solution.

We used 2D NMR ROESY experiments to identify possible nuclear Overhauser effects (NOEs) between amide protons and aromatic H2 and H4/H6 protons of the xylylene spacer. We first measured ROESY spectra of the shorter oligomer **2** in $CDCl_3$ at −20°C because the signals of the phenyl group are well spread out in this compound (Fig. 2*d*). The ROESY maps turned out to be complicated by exchange phenomena. A mixing time of 300 ms is required to detect NOE correlations, but this time is long enough for significant exchange to occur between P-P/M-M and P-M isomers, despite the fact that exchange, overall, is slow on the NMR time scale. As a result, the amide protons of each species appear to correlate with the phenyl aromatic protons of both species (not shown), making interpretations impossible.

Helix inversion is much slower in the longer oligomer **1**, and no exchange was observed in ROESY experiments with this compound. The most significant observation is that cross-peaks observed in the ROESY map measured at 25°C in toluene-d_8 indicate that the major P-P/M-M diastereomer is not fully folded as it is in the solid state. The central amide proton shows two correlations of different intensities: a strong correlation with the H2 phenyl proton and a weaker correlation with H4/H6 protons. The intensities of NOEs with H2 and H4/H6 protons are in a ratio of 3:1. The strong correlation with H2 is fully consistent with the conformations observed in the solid state (Fig. 3). However, the correlation with the H4/H6 protons is incompatible with this conformation and suggests that, in solution, rotations are allowed about NH–CH_2 and/or CH_2–phenyl bonds. A number of conformations of the xylylene spacer are compatible with P-P/M-M homochirality of the oligomer and with short distances between the central amide NH and H2 or H4/H6 phenyl protons. The conformations shown in Fig. 4 are those in which these distances are shortest and thus in which NOE correlations should have maximum intensities. These conformers are generated upon 180° rotations about CH_2–phenyl bonds. The spectrum of the major P-P/M-M diastereomer of **1** in solution presumably represents an average (fast equilibrium) between these species and all possible intermediates between them. The conformation of **1** observed in the solid state represents a significant population of P-P/M-M stereomers, but other conformers are populated as well.

Despite our efforts, little experimental data could be obtained about the minor P-M diastereomer. Its proportion in toluene-d_8 (<11%) is too weak to observe NOE correlations, and in $CDCl_3$, where its proportion is 50%, NMR signals of P-P/M-M and P-M

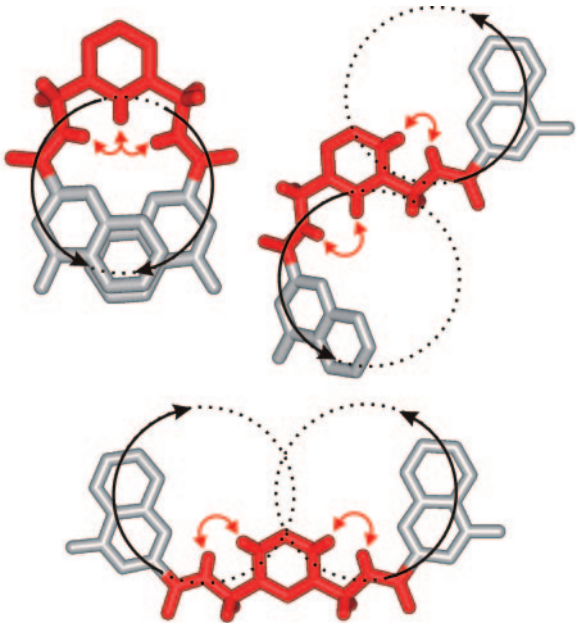

Fig. 4. Conformations of the central portion of **1** (or **2**) in which NOE correlations between H2, H4/H6, and NH protons have maximum intensities. The *meta*-xylylene unit is shown in red. NOEs are represented by red arrows. The dotted circles schematize the surfaces covered by the two helical segments. Overlap between the circles indicates possible steric hindrance between helices if they extend on the same side of the plane of the spacer. The black arrows indicate the direction along which each oligomeric segment extends from the spacer. The helices are located on the same of the plane of the spacer when both arrows turn in the same direction for P-P/M-M helices and when both arrows turn in opposite directions for P-M helices.

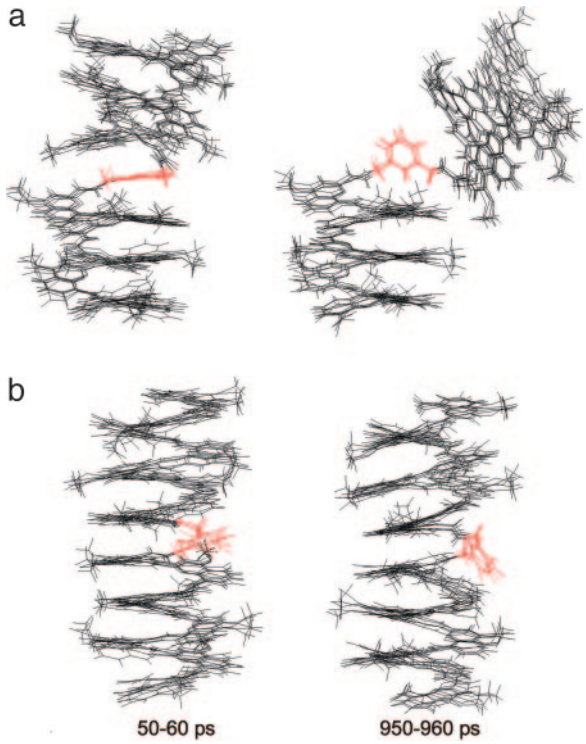

Fig. 5. Molecular dynamics simulation of **1** at 300 K in its P-M (*a*) and P-P (*b*) conformations. Superimposition of the five structures stored every 2 ps and sampled at the beginning and end of the simulation are shown in *Left* and *Right*, respectively. The *meta*-xylylene unit is shown in red.

species overlap. To explore the conformations at the helix inversion center, we turned to molecular dynamics studies of the P-P and P-M diastereomers of **1** (Fig. 5). These simulations suggest that intramolecular aromatic stacking endows P-P homochiral helices with a better structural integrity than those of the P-M *meso*-helices. At 300 K, the two helical segments of the P-P stereomer remain stacked during a 1-ns simulation (Fig. 5*b*), whereas they do not in the P-M diastereomer (Fig. 5*a*). In the latter case, the P and M segments do keep their helical integrity, but they completely lose contact after ≈500 ps. The largest conformational changes take place at the xylylene spacer: in particular, at aryl-CH_2 linkages. Even in the more stable P-P stereomer, the phenyl ring constitutes the most mobile part of the helix as it flips up and down to reach conformations where it lies almost parallel to the helix axis (see the supporting information).

We performed additional simulations of the P-P stereomer at higher *in silico* temperatures (400, 500, and 600 K), which, to some extent, is equivalent to simulating much longer periods. In all cases, the phenyl ring constitutes the most mobile part of the molecule despite its location at the center of the structure. At 600 K, conformational changes are such that the two helical segments eventually lose contact, as they do at 300 K for the P-M stereomer. This conformational change is presumably the first step toward the conversion of a P-P helix to a P-M diastereomer and certainly the first step to reach conformations as those shown in Fig. 4. These simulations are fully consistent with experimental data. They suggest that the inversion occurs preferentially at monomers having lower helix propensity and that, in the case of **1**, P-P/M-M homochiral helices should be stabilized in media that enhance aromatic stacking.

A comparison of solid-state structures and structures observed during molecular dynamics simulations reveals significant differences. In the crystal, the *meta*-xylylene unit is only slightly tilted out of the plane of the two adjacent quinolinecarboxamide rings. Torsion angles within the backbone of the helical segments are all <10° and reach 18° at the aryl-CH_2-NH linkages. At each methylene group, one C–H bond is almost perpendicular to the phenyl plane, and the other is perpendicular to the amide plane (Fig. 6*a*). The central amide protons and phenyl H2 are not exactly as represented in Fig. 4 but are still very close in space.

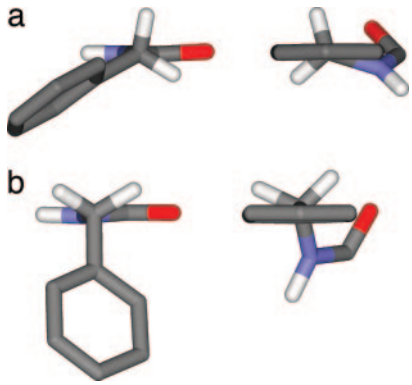

Fig. 6. Conformations of benzylamide groups. (*a*) Two views of the conformation of the benzylamide unit as seen in the solid-state structure of **2** showing that C^{α}–H bonds are almost perpendicular to the aryl plane (*Right*) or to the amide plane (*Left*). (*b*) Representative conformations of the benzylamide unit observed during molecular dynamics simulations of **1** (both P-P and P-M diastereomers) showing that the C^{α}–N bond (*Right*) and the C^{α}–C_{aryl} bond (*Left*) are almost perpendicular to the aryl plane and to the amide plane, respectively. Hydrogens are shown in white, carbons are shown in gray, nitrogen is shown in blue, and oxygens are shown in red. Hydrogens of the phenyl ring have been omitted for clarity.

When taking this conformation as the starting structure of a molecular dynamics simulation, large conformational changes occur at the xylylene spacer. The CH_2–N bond and the CH_2–C_{aryl} bond are almost perpendicular to the aryl plane and to the amide plane, respectively (Fig. 6*b*). Torsion angles about the aryl-CH_2-NH linkages remain at values near 60°. Clearly, the conformation at the xylylene units reflects the influence of several parameters. Intramolecular aromatic stacking above and below the xylylene unit as observed in the compact solid-state conformation certainly influences torsion angles about C^{α}–N and C^{α}–C_{aryl} bonds. The intrinsic conformational preferences of these bonds, which also define the helix propensity of this monomer, result from a combination of steric, electrostatic, and hyperconjugation effects as calculated for smaller benzylic structures (24, 25).

Conclusion

We have presented a simple strategy to study helix reversal phenomena within helical oligomers and to assess helix propensity of a given monomer within a particular structural context. When a monomer having a low helix propensity is placed between two stable helical segments, helix reversion occurs preferentially at this site, leading to the formation of P-P/M-M and P-M isomers, the proportion of which gives a direct measure of helix propensity. From this, it may be extrapolated whether an oligomer or a polymer containing a few or even many of these monomers should remain helically folded. This strategy has allowed us to characterize a species with a helix reversal located at a specific position in the helical chain. In QCOs possessing a *meta*-xylylene unit, inversion of helix handedness occurs up to 50% at this site in chloroform solutions; it is reduced to 10% in toluene and to 0% in the solid state. These results allow us to predict that oligomers composed of alternating *meta*-xylylenediamine and 2,6-pyridinedicarbonyl units are unlikely to fold into helices in solution. We expected a carboxylic acid anhydride spacer within QCOs to show little preference between P-P/M-M or P-M helicity. On the contrary, this monomer proved to have a high helix propensity and a strong preference for homochiral helicity. This result suggests that a polyanhydride composed of 2,6-pyridinedicarbonyl units should be helical.

This work was supported by the Conseil Régional d'Aquitaine, a Centre National de la Recherche Scientifique predoctoral fellowship (to C.D.), and the French Ministry of Research.

1. Green, M. M., Park, J.-W., Sato, T., Teramoto, A., Lifson, S., Selinger, R. B. L. & Selinger, J. (1999) *Angew. Chem. Int. Ed.* **38,** 3138–3154.
2. Hill, D. J., Mio, M. J., Prince, R. B., Hughes, T. S. & Moore, J. S. (2001) *Chem. Rev.* **101,** 3893–4011.
3. Nakano, T. & Okamoto, Y. (2001) *Chem. Rev.* **101,** 4013–4038.
4. Cornelissen, J. J. L. M., Rowan, A. E., Nolte, R. J. M. & Sommerdijk, N. A. J. M. (2001) *Chem. Rev.* **101,** 4039–4070.
5. Schmuk, C. (2003) *Angew. Chem. Int. Ed.* **42,** 2448–2452.
6. Yashima, E., Maeda, K. & Nishimura, T. (2004) *Chem. Eur. J.* **10,** 42–51.
7. Huc, I. (2004) *Eur. J. Org. Chem.* 17–29.
8. Clayden, J., Lund, A., Vallverdú, L. & Helliwell, M. (2004) *Nature* **431,** 966–971.
9. Spek, E. J., Gong, Y. & Kallenbach, N. R. (1995) *J. Am. Chem. Soc.* **117,** 10773–10774.
10. Guenet, J. M., Jeon, H. S., Khatri, C., Jha, S. K., Balsara, N. P., Green, M. M., Brûlet, A. & Thierry, A. (1997) *Macromolecules* **30**, 4590–4596.
11. Mutter, M., Tuchscherer, G. G., Miller, C., Altmann, K.-H., Carey, R. I., Wyss, D. F., Labhardt, A. M. & Rivier, J. E. (1992) *J. Am. Chem. Soc.* **114,** 1463–1470.
12. Ghadiri, M. R., Soares, C. & Choi, C. (1992) *J. Am. Chem. Soc.* **114,** 825–831.
13. Suzuki, K., Hiroaki, H., Kohda, D., Nakamura, H. & Tanaka, T. (1998) *J. Am. Chem. Soc.* **120,** 13008–13015.
14. Lifson, S. F., Felder, C. E. & Green, M. M. (1992) *Macromolecules* **25,** 4142–4148.
15. Jiang, H., Léger, J.-M. & Huc, I. (2003) *J. Am. Chem. Soc.* **125,** 3448–3449.
16. Jiang, H., Léger, J.-M., Dolain, C., Guionneau, P. & Huc, I. (2003) *Tetrahedron* **59,** 8365–8374.
17. Jiang, H., Dolain, C., Léger, J.-M., Gornitzka, H. & Huc, I. (2004) *J. Am. Chem. Soc.* **126,** 1034–1035.
18. Maurizot, V., Dolain, C., Léger, J.-M., Guionneau, P. & Huc, I. (2004) *J. Am. Chem. Soc.* **126,** 10049–10052.
19. Dolain, C., Jiang, H., Léger, J.-M., Guionneau, P. & Huc, I. (2005) *J. Am. Chem. Soc.* **127,** 12943–12951.
20. Dolain, C., Grélard, A., Laguerre, M., Jiang, H., Maurizot, V. & Huc, I. (2005) *Chem. Eur. J.* **11,** 6135–6144.
21. Green, M. M., Reidy, M. P., Johnson, R. J., Darling, G., O'Leary, D. J. & Willson, G. (1989) *J. Am. Chem. Soc.* **111,** 6452–6454.
22. Pearson, R. G. (1989) *J. Org. Chem.* **54,** 1423–1430.
23. Sugiura, H., Nigorikawa, Y., Saiki, Y., Nakamura, K. & Yamaguchi, M. (2004) *J. Am. Chem. Soc.* **126,** 14858–14864.
24. Avalos, M., Babiano, R., Barneto, J. L., Cintas, P., Jiménez, J. L. & Palacio, J. C. (2001) *J. Org. Chem.* **66,** 7275–7282.
25. Benassi, R. & Taddei, F. (1997) *J. Mol. Struct. (Theochem)* **418,** 59–71.